Coherent Change Detection Performance Using High-resolution SAR Images

Azzedine Bouaraba[1], Marc Acheroy[2] and Damien Closson[2]
[1]École Militaire Polytechnique, Algeria
[2]Royal Military Academy, Belgium

Abstract

In Coherent Change Detection (CCD) technique, the coherence between two Synthetic Aperture Radar (SAR) images is evaluated and analyzed to detect ground changes. With the recent upcoming of satellite constellations, that deliver high-resolution SAR images, it becomes possible to detect ground changes with fine spatial details and with a short temporal baseline. This aspect makes the CCD technique ideal for use in military and scientific applications such as border security and environmental monitoring. Unfortunately, the coherence estimator is biased, especially for low-coherence values. The space-averaged magnitude and complex coherence have been proposed in the past as efficient methods of bias removal when using medium-resolution SAR images. In this work, we are interested by the evaluation of the change detection performance improvements obtained by these two methods of bias removal when using high-resolution SAR images. Receiver Operating characteristic (ROC) curves have been experimentally evaluated using a pair of TerraSAR-X images. It is shown that in case of highly biased coherence, an additional improvement of change detection performance of about 15% can be obtained by the space-averaged complex coherence compared to the space-averaged coherence magnitude. When using large number of samples to estimate coherence, the two methods provide the same detection performance.

1. Introduction

Change detection using repeat-pass SAR images is one of the most important applications of remote sensing technology [1]-[4]. In CCD technique, the coherence between two SAR images is evaluated and analyzed to detect ground changes. Several methods have been proposed to enhance the coherence estimation [5]-[9]. In [7], a method of interferometric phase flattening has been presented to improve the coherence between SAR images. This technique can clarify the low coherence area due to the terrain change by improving coherence in the unchanged area.

With the recent upcoming of satellite constellations, that deliver high-resolution SAR images, it becomes possible to detect ground changes with fine spatial details and with a short temporal baseline. Unfortunately, the sample coherence estimator is biased, especially for low-coherence values. In [4], the accuracy of coherence estimation has been investigated as a function of the coherence map resolution. In addition to the presence of speckle in SAR data [10], the consequence of this bias is the appearance of highly coherent pixels inside the changed areas. Within this context, the change detection performance degrades considerably which complicates more the CCD map interpretation particularly when using high-resolution SAR data.

Medium resolution SAR images obtained from satellites such as ERS, Envisat and Alos involve the complex multilooking operation to square the pixels. This operation leads to the improvement of the coherence estimation but at the expense of the spatial resolution. Multilooking is not necessary when using high resolution SAR data such as Cosmo-SkyMed and TerraSAR-X since the image pixels are already nearly square. Nevertheless, the speckle is more noticeable in high-resolution data and the coherence bias is more important.

After coherence estimation stage, a simple threshold applied to the coherence image may be used to distinguish between the changed and unchanged regions in the scene. The detection performance of the thresholding method is low which is caused by the highly coherent pixels inside the changed areas [9]. The results may be improved with increasing values of the number of samples used to estimate the coherence [4]. Furthermore, a method for reducing the bias was proposed, based on space-averaging of sample coherence over an *M*-pixel local area [4]. This method allows also the enhancement of the probability of detecting ground changes, but at the expanse of the spatial resolution [9].

In SAR interferometry, the interferometric phase is stored along with the coherence magnitude. After flat-earth phase removal, the interferometric phase measures both topography and any changes in the apparent radar range. Then space-averaged complex coherence, compared to space-averaged coherence

magnitude, can offer an additional improvement of the change detection performance.

In the present work, we will attempt to quantify these additional improvements, in terms of probabilities of detection and false alarm when using high-resolution TerraSAR-X images. The test site concerns part of the maritime commercial port of Zeebrugge (Belgium) and the SAR data were acquired in spot-light mode.

The rest of the paper is organized as follows. In Section 2, the interferometric coherence and the two methods based on space-averaging of coherence samples are presented. Section 3 is devoted to the CCD application using experimental SAR data. The evaluation and the analysis of the change detection improvements that are obtained by the two applied methods are presented. The conclusion is given at the final section.

2. Coherence estimation and bias removal

2.1. InSAR Coherence

In order to provide some measure of discrimination in the SAR image pair and to accommodate the random noise fluctuations, the coherence is commonly used. The sample coherence, which is defined as the magnitude of the estimated sample complex cross-correlation coefficient between the SAR image pair, encodes the degree of scene similarity as a value in the range [0, 1][5]:

$$\gamma_N e^{j\phi} = \frac{\sum_{i=1}^{N} f_i \, g_i^*}{\sqrt{\sum_{i=1}^{N} |f_i|^2 \sum_{i=1}^{N} |g_i|^2}} \qquad (1)$$

where γ_N is the sample coherence obtained by N measurements, and ϕ is the SAR interferometric phase.

As shown in [1], the coherence is affected by different contributions which are mainly related to:

1. the relative backscatter signal to radar receiver noise ratio in the interferometric image pair,
2. the baseline decorrelation that is related to the satellite tracks separation, and
3. the temporal decorrelation caused by changes in the land surface, e.g., man-made objects, vegetation change or ploughing. It is the dominant factor in the repeat pass SAR interferometry [3], especially in flat terrain with low vegetation density.

As demonstrated in [4], the coherence estimator is biased especially for low coherence values. The bias is due to the limited sample size (N measurements) in the numerical computation of the Estimate (1).

2.2. Space-averaged coherence magnitude

A simple threshold applied to the coherence magnitude may be used to distinguish between the changed and unchanged regions in the scene. This method offers low-detection performances because of the biased coherence estimator, especially for low values [9]. In order to improve the detection performances, the basic space-averaging operation over M-pixel local area is commonly performed [4]:

$$z_1 = \frac{1}{M} \sum_{i=1}^{M} \gamma_{Ni} \begin{matrix} \geq T_1 & (H_0) \\ \prec T_1 & (H_1) \end{matrix} \qquad (2)$$

where H_0 is a realization of the null hypothesis (scene changes of interest absent) and H_1 is the alternative hypothesis (scene changes of interest present).

2.2. Space-averaged complex coherence

According to Equation 1, the SAR interferometric phase is stored along with the sample coherence magnitude. After flat-earth phase removal, this interferometric phase measures both topography and any changes in the apparent radar range. In the following, spatial averaging over an M-pixel local area is done using both magnitude and phase of the N-look samples of complex coherence [4]:

$$z_2 = \frac{1}{M} \left| \sum_{i=1}^{M} \gamma_{Ni} \, e^{j\phi_i} \right| \begin{matrix} \geq T_2 & (H_0) \\ \prec T_2 & (H_1) \end{matrix} \qquad (3)$$

To decide whether the pixel under test corresponds to hypothesis H_0 or H_1, the statistics z_1 and z_2 are compared to a given threshold value $T_{i=1,\,2}$ [9]. These two methods were developed in [4] and both proposed as coherence bias removal. In the following section, we attempt to quantify experimentally the change detection performance improvements obtained by the two statistics z_1 and z_2.

3. Application to experimental SAR data

The results presented in this work are obtained with SAR data in X-band, horizontally polarized in spot-light mode. The TSX images are acquired on 15 and 26 June 2011, with an incident angle of 42°. The pixel resolution is 1 m in both ground range and azimuth directions. The test site, shown in Figure 1 (a), is part of the maritime commercial port of Zeebrugge, Belgium. The coregistration of the SAR images was performed with Sarscape software (Sarmap™ 2012). Developments were carried out in IDL (Interactive Data Language).

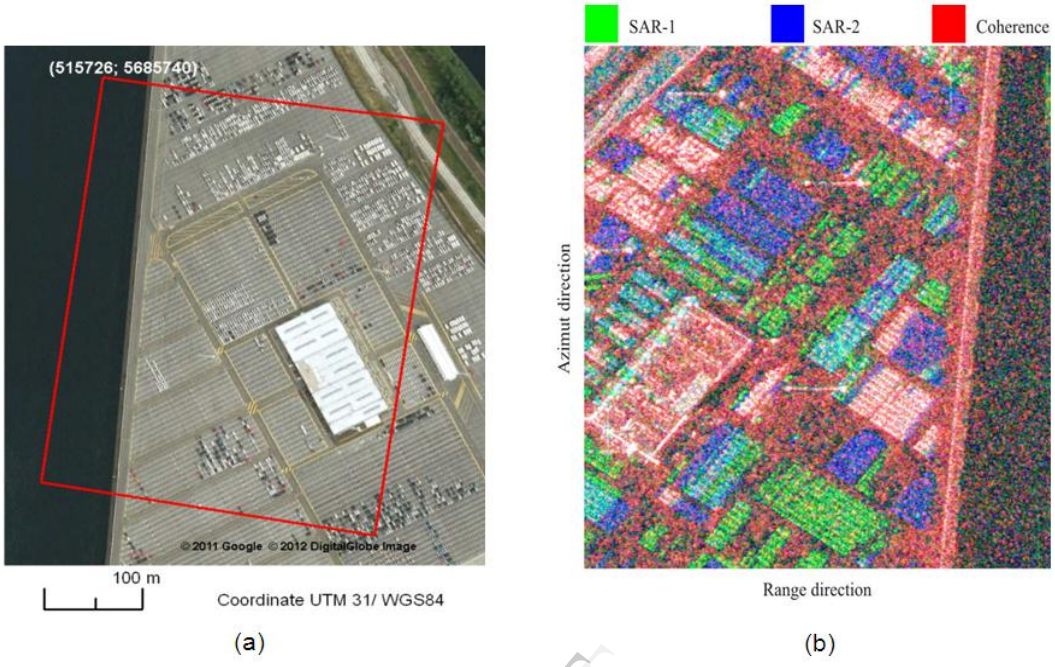

Figure 1. (a) Optical image from Google Earth of the test site corresponding to part of commercial port of Zeebrugge (Belgium). The rectangle indicates the area of interest corresponding to the used SAR images sub-set size of 500×500 pixels. **(b)** Color composition of the coherence magnitude image (red color) and the two TerraSAR-X acquisitions of June 15 (green color) and 26 (blue color), 2011. Light-colored pixels indicate scatterers existing in both acquisitions and characterized by high coherence value.

Figure 1 (b) shows the two intensity images and the coherence map of the test site. The coherence is obtained using 3×3 sliding estimation window. Red colored pixels represents the undisturbed areas while absence of red color represents the changed area (example of the sea area at the right side of Figure 1 (b)). Green-colored pixels show the scatterers present only in the first acquisition of 15 June 2011. Similarly, blue-colored pixels indicate scatterers detected only in the second acquisition of 26 June 2011. One can see that most of the changes, which are occurred between two images, correspond to the displacements of containers and vehicles on the terminal port area. Light-colored pixels indicate scatterers existing in both acquisitions and characterized by high coherence value. This corresponds mostly to undisturbed containers or vehicles and to the permanent structures such as the big hangar visible inside the rectangle in Figure 1 (a).

To evaluate experimentally Receiver Operating characteristic (ROC) curves, the selection of the changed and unchanged areas must be done carefully. The advantage of using high-resolution SAR data is that it is possible to select a large unchanged area (of 140×140 pixels in the present work), characterized by a high-coherence (mean value of about 0:85).

The selection of changed area is made easy when using SAR data in X-band because a subtle change on surface allows for a decorrelation in the coherence image (see Figure 1 (b).). Here, the changed area has been chosen inside the sea with sub-set size of 500×500.

Figure 2 depicts histograms of coherence images, obtained by using TSX data, evaluated for different number of samples (N). It can be seen the high number of coherent pixels inside the changed caused by the coherence bias. The coherence bias decreases with increasing number of samples used to estimate the coherence. For example, the coherence evaluated by using $N = 5\times5$, compared to that evaluated by $N = 3\times3$, represents more faithfully the coherence of changed area because there are less samples of high coherence inside the changed area. According to Figure 2, the coherence mean value of the selected changed area is 0:31 for $N = 25$ against 0:47 for $N = 9$. The decreases of number of highly coherent pixels inside the changed area, caused by the presence of bias in the coherence

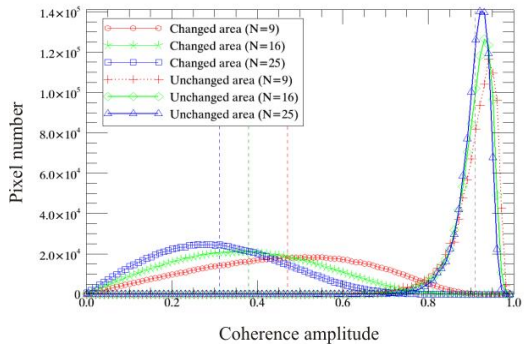

Figure 2. Histograms of the selected changed and unchanged areas coherences using different number of samples *N*. The bias of coherence estimate, that affect particularly the low values, decreases with increasing *N*.

estimate, permit an important increasing of change detection performance.

Not that coherence histograms of the changed area correspond to the same selected area (sea) and the difference is only due to the increasing number of samples. This is not the same in case of the selected unchanged area, where the coherence mean value is not affected (at least slightly changed) by increasing *N*.

According to Figure 2, the coherence mean value of the unchanged area is about 0:92 for the different values of *N* (9, 16 and 25). This may be explained by the fact that the coherence estimate is only biased for the low values.

The analysis of Figure 2 shows the importance of good estimation of the coherence by increasing number of samples, but using a high value of *N* causes also the loss of subtle changes in the coherence image. For that reason, the use of space-averaged coherence over an *M*-local areas is required to enhance the change detection performance while preserving detection of the subtle changes. Not that results presented in Figure 2 agree with the theoretical results of [4].

The space-averaged complex coherence uses the multilook (*N*-look) of the interferometric phase (Equation 1). In the present work, the best detection performance, in terms of probabilities of detection and false alarm, is obtained using the flattened interferometric phase filtered by the Goldstein filter, instead of the simple mean filter, with a window size of *N* pixels.

Figure 3 shows the flattened and filtered interferometric phase obtained by TSX image acquisitions of 15 and 26 June 2011. One can see that this phase measures both topography and any changes in the apparent radar range. By comparing to the

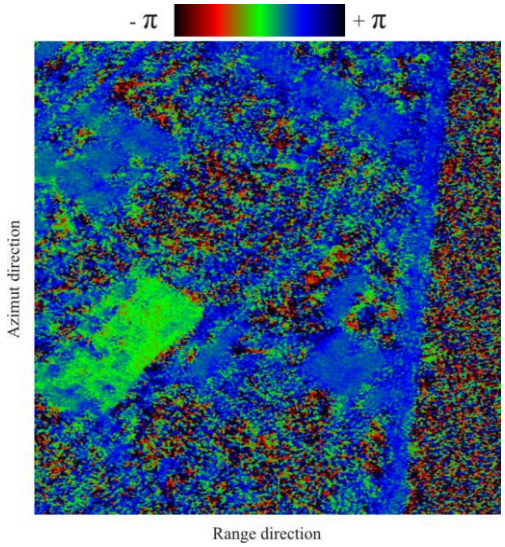

Figure 3. Flattened and filtered interferometric phase obtained by the TSX acquisitions of 15 and 26 June 2011.

coherence image shown in Figure 1 (b), we notice that for the changed area (example of sea at the right side of the image), the corresponding phase is random uniformly distributed. For an unchanged area (light-colored pixels in Figure 1 (b)) the corresponding SAR interferometric phase values are quite steady. This means that when evaluating the statistic z_2, comparing to z_1, we obtain low values for changed areas because of the incoherent summation of the complex coherence samples (random phase). For the unchanged areas, the statistic z_2 will be quite similar to z_1 (coherent summation of the complex coherence samples). In this case, the contrast is accentuated between coherence of changed and unchanged areas. In other words, the space-averaging of the complex coherence samples leads to an improvement of the change detection performance. In the following paragraphs we attempt to quantify the improvement in terms of probability of detection and false alarm.

3.1. Experimental ROC evaluation

The detection performance may be quantified by evaluating the probability of detection P_d and the corresponding false alarm P_{fa} [5]:

$$P_d = \int_0^T P(\hat{\gamma}|\gamma = \gamma_{changed})\, d\hat{\gamma} \qquad (4)$$

$$P_{fa} = \int_0^T P(\hat{\gamma}|\gamma = \gamma_{unchanged})\, d\hat{\gamma} \qquad (5)$$

The procedure used to estimate experimentally *Pd* and *Pfa* is based on Equations 4 and 5. To evaluate *Pd*,

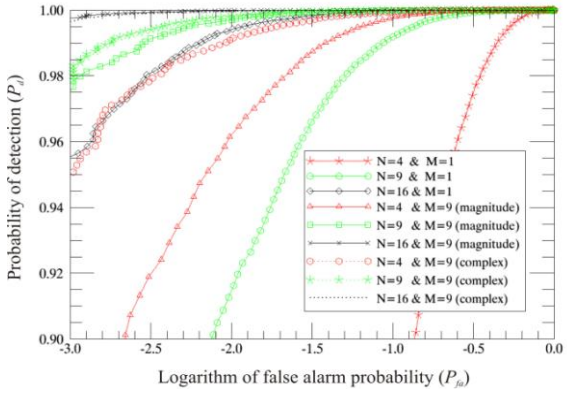

Figure 4. Experimental ROC curves, corresponding to different parameters values M and N, obtained by the TSX acquisitions of 15 and 26 June 2011.

the pixel under test is set in the middle of moving window (size of *M*), which is sliding to scan all coherence data of the selected changed area. The actual P_d is then given by the ratio of the total number of times the test, given by Equation (2) or (3), exceeds the threshold *T* and the total number of data in the selected changed area (500×500 pixels). Similarly, the probability of false alarm P_{fa} can be evaluated in the same way as P_d using the coherence data in the selected unchanged area. P_{fa} is then given by the ratio of the total number of times the test exceeds the threshold *T* and the total number of data in the selected unchanged area (140×140 pixels). For low values of *T*, P_{fa} is low, but the P_d will be also low and insufficient to detect all changes. For high values of *T*, both P_d and P_{fa} will be high. We select typically a threshold that offers high (sufficient) P_d and at the same time gives an acceptable false alarm value.

The ROC curves are defined as plots of P_d versus P_{fa} and are generated by varying detector threshold *T*. These curves are established using the two areas (selected changed and unchanged area) as ground truth and the probabilities P_d and P_{fa} are determined for the two methods of space-averaging coherence, complex and magnitude, according to different values of parameters *M* and *N*.

Figure 4 depicts the ROC curves evaluated for different values of *N* (4, 9 and 16) and *M* (1 and 9). One can see that the ROC curve corresponding to parameters $N = 4$ and $M = 1$ has the lowest performance and a great improvement can be obtained

Parameters	$M = 1$	$M = 9$ (Magnitude)	$M = 9$ (Complex)
$N = 4$	$P_d = :280$	$P_d = :822$	$P_d = :951$
$N = 9$	$P_d = :728$	$P_d = :975$	$P_d = :983$
$N = 16$	$P_d = :956$	$P_d = :997$	$P_d = :996$

Table 1. Detection probabilities *Pd* obtained by TSX data for the same false alarm rate $Pfa = 10^{-3}$.

by space-averaged coherence magnitude when using a window-size $M = 9$. Further improvements can also be obtained from space-averaged complex coherence of about 15% detection probability (according to Table 1) in case of false alarm value of $P_{fa} = 10^{-3}$. This value of false alarm corresponds to the simple thresholding method ($M = 1$) of the coherence magnitude evaluated by using $N = 16$ samples with a threshold value of $T = 0{:}75$, which correspond to the intersection of changed and unchanged coherence histograms (see Figure 2).

Figure 4 shows that, for high values of *N* and *M*, the detection performances are practically identical between those obtained by space-averaged complex coherence and coherence magnitude. In this work, we found that for $N= 12$, there is no significant improvement beyond $M=9$ (and conversely, for $N=9$, no significant improvement beyond $M = 12$). In this case, the two methods (space-averaged coherence magnitude and complex) provide the same detection performance.

3.2. CCD results analysis

Figure 5 depicts results of CCD obtained by the two methods of space-averaged coherence (complex and magnitude). These results correspond to the different parameters values *N* and *M* of Table 1. The CCD result obtained for $N = 4$ and $M = 1$, see Figure 5 (a), is not exploitable because insufficient number of samples are used to estimate coherence.

An enhancement of the result can be achieved by space-averaging coherence magnitude with $M = 9$ (see Figure 5 (b)). In this case, with the same parameter values *M* and *N*, an additional improvement can also be obtained only by space-averaging complex coherence. This result, see Figure 5 (c), is comparable to thus obtained by space-averaged coherence magnitude with $N = 16$ and $M = 1$ (see Figure 5 (g)).

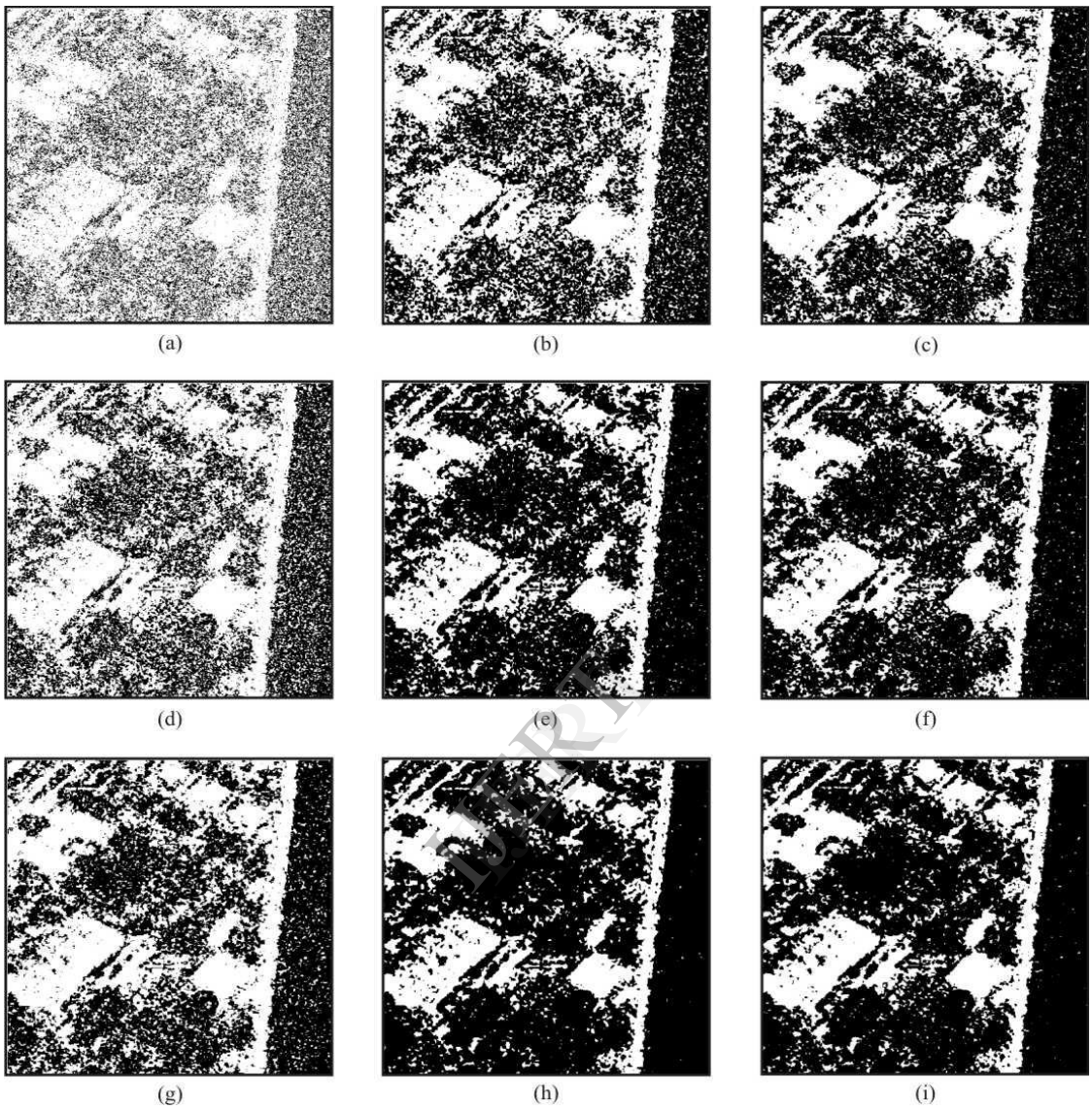

Figure 5. CCD maps obtained using the two TSX acquisitions of 15 and 26 June 2011. Dark pixels indicate detected changed area while white pixels indicate unchanged area. Images are shown at a fixed P_{fa} of 10^{-3}. (a) CCD map for N=4 and M=1. (b) CCD (magnitude) map for N=4 and M = 9. (c) CCD (complex) map for N = 4 and M = 9. (d) CCD map for N = 9 and M = 1. (e) CCD (magnitude) map for N = 9 and M = 9. (f) CCD (complex) map for N = 9 and M = 9. (g) CCD map for N = 16 and M = 1. (h) CCD (magnitude) map for N = 16 and M = 9. (i) CCD (complex) map for N = 16 and M = 9.

When two methods offer the same detection performance, it is recommended to choose the one that uses the smallest window-size, in order to detect subtle details.

The detection performance improves with increasing N, and additional improvements can be obtained by space-averaged coherence with M = 9 (see Figure 5 (h) and (i)). In this case, the two methods of space-averaged coherence (complex and magnitude) offer the same detection performances. This may be explained by the fact that the coherence bias is highly reduced beyond sufficient number of samples (N = 12 and M =9 in this work) and then the coherence magnitude estimates faithfully the true scene coherence.

4. Conclusion

In this study, an evaluation of change detection performance improvements obtained by two methods of coherence bias removal is performed. High resolution TerraSAR-X images are used to quantify the change detection improvement in terms of probabilities of detection and false alarm. The results show that when using a small number of samples to evaluate coherence (case of highly biased coherence) an important additional improvement (about 15%) of change detection performance can be obtained by space-averaging complex coherence compared to space-averaging of only coherence magnitude. When increasing the number of samples, used to evaluate coherence, and beyond a certain limit of spatial window size, it has been shown that there is no additional improvement and the two methods (space-averaging coherence magnitude and complex values) provide the same detection performance.

5. Acknowledgment

The authors would like to thank the private companies Sarmap and EXELisvis for their support in providing a full Sarscape license (v.4.8, 2011). The TerraSARX data were processed at the Royal Military Academy of Belgium.

6. References

[1] H. A. Zebker, "Decorrelation in interferometric radar echoes," *IEEE Trans. Geosci. Remote Sens.*, Vol. 30, No. 5, 950–959, 1992.

[2] E. J. Rignot, "Change detection techniques for ERS-1 SAR data," *IEEE Trans. Geosci. Remote Sens.*, Vol. 31, No. 4, 896–906, 1993.

[3] D. G. Corr, " Coherent change detection of vehicle movements," *in Proc. IGARSS.*, Vol. 5, 2451–2453, 1998.

[4] R. Touzi, "Coherence Estimation for SAR Imagery," *IEEE Trans. Geosci. Remote Sens.*, Vol. 37, No. 1, 135–149, 1999.

[5] M. Preiss, "Detecting scene changes using synthetic aperture radar interferometry," *IEEE Trans. Geosci. Remote Sens.*, Vol. 44, No. 8, 2041–2054, 2006.

[6] R. Sabry, "A New Coherency Formalism for Change Detection and Phenomenology in SAR Imagery: A Field Approach," *IEEE Geosc. and Remote Sens. Letters*, Vol. 6, No. 3, 458–462, 2009.

[7] N. Oishi, "A Coherence Improvement Technique for Coherent Change Detection in SAR Interferometry," *In Proc. of the 6th European Radar Conference*, Rome, Italy, 2009.

[8] R. G. Phillips, "Clean: A false alarm reduction method for sar ccd," *Speech and Signal Processing (ICASSP)*, 1365–1368, 2011.

[9] A. Bouaraba, "Robust techniques for coherent change detection using Cosmo-skymed SAR images," *Progress In Electromagnetics Research M*, Vol. 22, 219–232, 2012.

[10] C. L. Martinez, "Coherence estimation in synthetic aperture radar data based on speckle noise modeling," Applied Optics, Vol. 46(4):544–558, 2007.